Multiple dopplerons in aluminum

V. G. Skobov, L. M. Fisher, A. S. Chernov, and V. A. Yudin

Moscow Engineering-Physics Institute
All-Union Electro-technical Institute
(Submitted April 26, 1974)
Zh. Eksp. Teor. Fiz. 67, 1218–1232 (September 1974)

Doppler-shifted cyclotron resonance (DSCR) is investigated in aluminum. The impedance of a plate in a magnetic field **H** parallel to the [100] axis oriented perpedicular to the sample surface is investigated experimentally and theoretically. Circular polarizations of the exciting radio-frequency field are used in the experiment. Besides the helicon oscillations of the surface-resistance derivatives $dR_{\pm}/dH$ as functions of the magnetic field intensity, a series of oscillations with multiple periods are observed. Some properties of the oscillations, viz., their existence for only certain circular polarizations, the limited range of the magnetic field strength, and the field dependence of the periods, indicate that they are due to the propagation of dopplerons due to multiple DSCR but not to the Gantmakher–Kaner size effect. A theoretical analysis is carried out for a simple model Fermi surface possessing fourfold symmetry with respect to the [100] axis and describing qualitatively the shape and size of the real Fermi surface. It is shown that multiple dopplerons with definite circular polarization should exist in aluminum. The theory and experiments are in qualitative agreement. Our simple model predicts most of the features of DSCR in aluminum.

1. INTRODUCTION

As is well known, the Doppler shifted cyclotron resonance (DSCR) of conduction electrons manifests itself in the appearance of thresholds for collisionless cyclotron absorption of electromagnetic waves in metals. The DSCR leads to a limitation of the region of existence of helicons in uncompensated metals [1], and to the Gantmakher-Kaner size effect [2]. In addition, the DSCR gives rise to the appearance of new propagating modes [3,4]. In [5,6], with simple Fermi-surface models as examples, it was demonstrated that excitation of the DSCR modes, which were later called dopplerons, should lead to oscillations of the impedance of a plate, similar to Gantmakher-Kaner oscillations (GKO). It has been shown [7-10] that the surface-resistance oscillations observed in cadmium, indium, and copper are due to excitation of dopplerons. In cadmium, the dopplerons are due to the electrons and holes with maximum displacement during the cyclotron period [7]. The wave fields of these dopplerons rotate in the same direction as the corresponding carriers [7,8]. In indium [9] and in copper [10], the dopplerons are due to the DSCR of the carriers having the minimal displacement per period, and their fields rotate in a direction opposite to the direction of rotation of these carriers.

The present paper is devoted to a study of DSCR in aluminum. The behavior of the impedance of an aluminum plate in a magnetic field **H** normal to the sample surface was investigated by a number of workers [11,12]. Series of oscillations were observed, with multiple periods, and were attributed to the Gantmakher-Kaner effect. The possibility that these oscillations result from dopleron excitation was also discussed [12], but the authors of [12] preferred the first of the foregoing explanations.

The present study was undertaken to ascertain the nature of the oscillations in aluminum. We investigated the impedance of a plate in a magnetic field **H** parallel to the [100] axis and oriented normal to the surface of frequency field of circular polarization. The use of circular polarizations has demonst ted that each of the series of oscillations in aluminum has a perfectly defined circular polarization. This proves that they are connected with the excitation of dopplerons, inasmuch as the GKO have linear polarization. The oscillations of the fundamental DSCR are observed both below and above the helicon threshold, and their circular polarization is opposite to that of the helicon. The polarization of the fifth harmonic coincides with the polarization of the fundamental resonance, while the polarization of the third harmonic coincides with the polarization of the helicon. The results agree with the conclusions of the theory. A theoretical investigation was carried out for a model Fermi surface having a fourfold symmetry. Therefore, unlike the previously considered [9,10] axially symmetrical models, in this model there exists multiple resonances and dopplerons that correspond to them.

2. THEORY

A. Fermi-surface Model

As is well known, the Fermi surface of aluminum consists of a large hole surface in the third Brillouin zone and a small group of electrons in the fourth zone [13]. The electron density is less than 3% of the hole density, so that the contribution of the electrons to the conductivity will be neglected in the study of the DSCR of the holes.

The hole surface has a fourfold symmetry relative to the principal axes of the crystal. Plots of the area $S(k_z)$ of the intersection of this surface with the plane k_z = const (k_z axis ∥ [100]) and of its derivative $\partial S/\partial k_z$, as functions of k_z, are shown in Fig. 1 by thin lines. These plots are the result of the calculation of Larsen and Greisen [11].

We consider a model in which the $S(k_z)$ dependence is described by the formulas

Copyright © 1975 American Institute of Physics

$$\frac{\partial S}{\partial k_z} = -\frac{\pi}{a} y\left(\frac{|k_z|a}{\pi}\right) \operatorname{sign} k_z, \tag{1}$$

$$y(x) = y_m \begin{cases} \dfrac{\alpha x}{x_1 - (1-\alpha)x}, & x < x_1 \\ \eta - \dfrac{\eta-1}{\beta}\left(\dfrac{1+\beta}{1-\zeta}\dfrac{x-x_3}{x_3} + 1\right)^2, & x_1 < x < x_2, \\ 1 + \dfrac{(\eta-1)(1+\beta)}{(1-\zeta)^2(1-\beta)}\left(\dfrac{x}{x_3} - 1\right)^2, & x_2 < x < x_3 \end{cases} \tag{2}$$

$$\alpha = \frac{\beta(1-\zeta)}{2(1+\beta)\zeta(\eta-1)}, \quad \eta = \frac{y_M}{y_m}, \tag{3}$$

$$x_1 = \zeta x_3, \quad x_2 = [\zeta + \beta(1-\zeta)]x_3.$$

At $x_3 < x < 2x_3$, the function $y(x)$ must be continued symmetrically with respect to the point $x = x_3$. In these formulas, a is the lattice constant, η is the ratio of the maximum value y_M of the function $y(x)$ to the value of y_m at the minimum at $x = x_3$. We choose y_m such that the limiting period of the doppleron oscillations coincides with the experimentally observed one. We note that the experimental results of [11,12], just as our measurements, yield larger values of $\partial S/\partial k_z$ at the minimum for real aluminum than in the theoretical model of Larsen and Greisen.

For a unique determination of the Fermi surface it is necessary also to specify the cross section area $S(0)$ at $k_z = 0$. We obtain this area from the condition that the density of the holes in the model be equal to the true density in aluminum:

$$N = \frac{x_3}{a^3}\left(\frac{a^2}{\pi^2}S(0) - \int_0^{x_3} y(x)\,dx\right). \tag{4}$$

For the quantities $a = 4.05$ Å, $N = 0.062$ Å^{-3}, and the parameters

$$y_m = 8.1, \quad \eta = 1.1, \quad x_1 = 0.154, \quad x_2 = 0.163, \quad x_3 = 0.700 \tag{5}$$

the plots of $S(k_z)$ and $\partial S/\partial k_z$ are shown in Fig. 1 by the thick curves. The $\partial S/\partial k_z$ plot in our model is symmetrical with respect to the minimum, and this greatly simplifies the calculations. The left-hand side of the $\partial S/\partial k_z$ plot is similar to the corresponding part of the Larsen and Greisen curve. On the other hand, the difference between the right-hand sides is insignificant, since most holes are in the region $|k_z| < x_3\pi/a$.

As the curve describing the boundary of the cross section of the Fermi surface we choose the astroid

$$k_x^{2/3} + k_y^{2/3} = [8S(k_z)/3\pi]^{1/3}. \tag{6}$$

Of course, this curve differs from the shape of the cross section of the real Fermi surface of aluminum. However, it does have a fourfold symmetry and is similar to the real cross section of the Fermi surface in the vicinity of the minimum of $\partial S/\partial k_z$. Therefore the behavior of the nonlocal conductivity near the DSCR due to the holes with the minimum value of $\partial S/\partial k_z$ is described qualitatively correctly by this model.

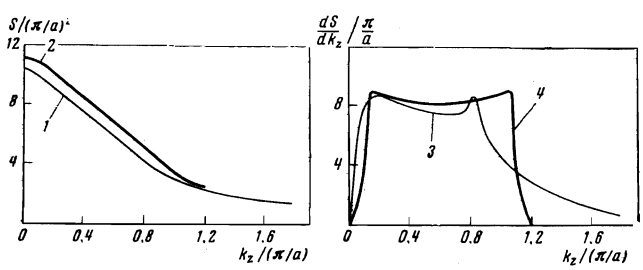

FIG. 1. Plots of the area (curves 1 and 2) and of the derivative of the area (curves 3 and 4) of the cross section of the Fermi surface of aluminum; $k_z \parallel [100]$.

The carrier dispersion law $\epsilon = \epsilon(\mathbf{k})$ for our model can be expressed in the form

$$2\pi\hbar^{-2}m\varepsilon(\mathbf{k}) - S(0) = {}^3/_8\pi(k_x^{2/3} + k_y^{2/3})^3 - S(k_z), \tag{7}$$

where m is the cyclotron mass. The Fermi energy is $\epsilon_F = \hbar^2 S(0)/2\pi m$. Indeed, at $\epsilon(\mathbf{k}) = \hbar^2 S(0)/2\pi m$ the left-hand side of (7) vanishes, and we obtain Eq. (6) for the cross section of the Fermi surface. With this dispersion law, the energies of the longitudinal and transverse motion enter additively, as the result of which the longitudinal carrier velocity v_z is independent of the transverse momentum components. This circumstance greatly simplifies the calculation of the nonlocal conductivity, and at the same time has no qualitative influence on the dispersion curves of the DSCR modes (according to Larsen and Greisen [11], allowance for the dependence of v_z on k_x and k_y leads to a change of the nonlocal conductivity by an amount on the order of 5%).

The equation describing the intersection of the equal-energy surface and the plane perpendicular to the magnetic field ($\mathbf{H} \parallel k_z$) can be conveniently expressed in parametric form

$$k_x = \rho\cos^3\varphi, \quad k_y = \rho\sin^3\varphi, \tag{8}$$

where φ is the azimuthal angle in the $k_z k_y$ plane. At $\epsilon = \epsilon_F$ we have

$$\rho^2 = 3S(k_z)/8\pi, \tag{9}$$

and Eqs. (8) are equivalent to Eq. (6). Differentiating $\epsilon(\mathbf{k})$ with respect to $\mathbf{k}$ and using (8), we obtain expressions for the hole velocity components:

$$mv_x = \frac{3\hbar\rho}{8\cos\varphi}, \quad mv_y = \frac{3\hbar\rho}{8\sin\varphi}, \quad mv_z = \frac{\hbar}{2\pi}\frac{\partial S(k_z)}{\partial k_z}. \tag{10}$$

B. Nonlocal Conductivity

The general expression for the elements of the conductivity tensor $\sigma_{\alpha\beta}(\kappa, \omega, \mathbf{H})$ is given, for example, in [14]. For circular polarizations, in the case considered by us, it can be transformed into

$$\sigma_\pm = \sigma_{xx} \pm i\sigma_{yx} = \frac{2\pi e^2\hbar m}{(2\pi\hbar)^3}\int dk_z \sum_{n=-\infty}^{\infty} \frac{v_n^\pm(v_n^+ + v_n^-)^*}{\nu + i(n\Omega - \kappa v_z - \omega)}, \tag{11}$$

where

$$v_n^\pm = \frac{1}{2\pi}\int_0^{2\pi}[v_x(\tau) \pm iv_y(\tau)]e^{in\tau}\,d\tau, \tag{12}$$

$\Omega = eH/mc$ is the cyclotron frequency of the holes, ω is the frequency of the electromagnetic wave, κ is the wave vector, and ν is the frequency of the carrier collisions with the lattice. We shall henceforth consider the case of strong magnetic fields, when $\Omega \gg |\nu - i\omega|$. The dimensionless time τ, which characterizes the motion of the particle along the orbit, is connected with the angle φ by the relation

$$d\tau = -\frac{\hbar}{m}\left[\frac{(dk_x)^2 + (dk_y)^2}{v_x^2 + v_y^2}\right]^{1/2} = -(1 - \cos 4\varphi)\,d\varphi. \tag{13}$$

Substitution of (10) in (12) with allowance for (13) leads to the following expression for the Fourier components of the transverse velocities:

$$v_{4s\pm1}^\pm = \frac{3\hbar\rho}{4m}\left[J_s\left(s \pm \frac{1}{4}\right) - J_{s\pm1}\left(s \pm \frac{1}{4}\right)\right], \quad s = \ldots, -2, -1, 0, 1, 2, \ldots, \tag{14}$$

where $J_s(x)$ is a Bessel function of order s. The remaining Fourier components of the transverse velocities, for a Fermi surface having fourfold symmetry, are equal to zero.

If we now substitute (14) and (9) in (11) and use the connection between v_z and $\partial S/\partial k_z$, then the expression for the nonlocal conductivity can be represented in the form

$$\sigma_\pm = -i\frac{Nec}{H}\sum_{s=-\infty}^{\infty}\frac{A_s^\pm}{4s\pm 1-i\gamma}\left[F\left(\frac{q}{4s\pm 1-i\gamma}\right)+F\left(\frac{-q}{4s\pm 1-i\gamma}\right)\right], \quad (15)$$

$$A_s^\pm = {}^3/_2[J_s(s\pm{}^1/_4)-J_{s\pm 1}(s\pm{}^1/_4)]^2, \quad (16)$$

$$F(p)=\frac{1}{2x}\int_0^{x_0}dx\left[1-p\frac{y(x)}{y_m}\right]^{-1}, \quad (17)$$

$$q=\frac{\varkappa u_{min}}{2\pi},\quad u_{min}=\frac{\pi\hbar c y_m}{eaH},\quad \gamma=\frac{\nu}{\Omega}. \quad (18)$$

The quantity q represents the ratio of the displacement u_{min} of the holes with $k_z = \pi x_3/a$ to the length of the electromagnetic wave. In (15) we assume that γ does not depend on k_z.

Direct calculation of the integral (17) yields

$$F(p)=I_1(p)+I_2(p)+I_3(p), \quad (19)$$

$$I_1(p)=\frac{\zeta}{2(1-\alpha+\alpha p)}\left[1-\alpha-\frac{\alpha p}{1-\alpha+\alpha p}\ln\alpha(1-p)\right], \quad (20)$$

$$I_2(p)=\frac{\beta(1-\zeta)}{2(1+\beta)[p(\eta-1)(1-p\eta)]^{1/2}}\operatorname{arctg}\frac{(1+\beta)[p(\eta-1)(1-p\eta)]^{1/2}}{1-p[\eta+\beta(\eta-1)]}, \quad (21)$$

$$I_3(p)=\frac{(1-\beta)(1-\zeta)}{4(1-p)^{1/2}[p(1-\beta^2)(\eta-1)]^{1/2}}\ln\frac{(1-p)^{1/2}+[p(1-\beta^2)(\eta-1)]^{1/2}}{(1-p)^{1/2}-[p(1-\beta^2)(\eta-1)]^{1/2}}. \quad (22)$$

The function $I_1(p)$ has a cut in the complex p plane, from p = 1 to p = +∞. At Re p > 1, this function must be calculated on the second sheet above or below the cut, depending on the sign of the imaginary part, which results from the collisions with the lattice, of the argument in (15). The function $I_2(p)$ has a cut in the p plane from $p = \eta^{-1}$ to p = 1, while the function $I_3(p)$ has a cut from $p = [\eta - \beta^2(\eta-1)]^{-1}$ to p = 1. The function $I_2(p)$ in the region $\eta^{-1} < \mathrm{Re}\, p < 1$ and the function $I_3(p)$ in the region $[\eta - \beta^2(\eta-1)]^{-1} < \mathrm{Re}\, p < 1$ are calculated in analogy with I_1.

The right-hand side of (15) is a sum of terms corresponding to the odd harmonics of the DSCR. The presence of multiple resonances at $s \neq 0$ is due to the fact that the Fermi surface has no axial symmetry.

The dependence of the function F on p is due to the spatial dispersion. When p varies from zero to η^{-1}, the function F increases monotonically from unity to infinity, remaining real and positive. The root singularity of I_2 as $p \to \eta^{-1}$ is due to the DSCR of the holes that have a maximum displacement $u_{max} = \eta u_{min}$. In the region $p > \eta^{-1}$, the function F acquires an imaginary part which describes the collisionless cyclotron absorption by the holes, the displacement of which is equal to the length of the electromagnetic wave. The imaginary part of F becomes infinite to the right of the point $p = \eta^{-1}$ and to the left of the point p = 1. Im F is small in the region p > 1. The real part of I_3, on the other hand, has a root singularity to the right of the point p = 1, which tends to minus infinity as $p \to 1$. This conductivity singularity is connected with the DSCR of holes having a minimum displacement u_{min} over the cyclotron period. With increasing p, the function Re F(p) increases, goes through zero at the point p = 2.33, and reaches a maximum Re F(0.03) = 0.048 at p = 3.03. With further increase of p, the function Re F(p), while remaining positive, tends monotonically to zero. The reversal of the sign of Re F(p) at p = 1 is due to the presence of the minimum of $\partial S/\partial k_z$ at $k_z = \pi x_3/a$. At p > 1, the main contribution to the nonlocal conductivity is made by holes with $k_z \sim \pi x_3/a$, the displacements of which are larger than the electromagnetic wavelength $2\pi/\kappa'$. The Doppler shift of the frequency $\kappa' v_z$ for these holes exceeds the cyclotron frequency, as a result of which the nonlocal hole conductivity reverses sign, i.e., the holes behave like the electrons in the wavelength region p > 1.

C. Solution of the Dispersion Equation

The properties of the electromagnetic waves in a metal are determined by the solutions of the dispersion equation

$$\varkappa^2c^2=4\pi i\omega\sigma_\pm(\varkappa,\omega,H).$$

Using the dimensionless variable q, it is convenient to represent this equation in the form

$$\omega_L/\omega=\Phi_\pm(q), \quad (23)$$

$$\Phi_\pm(q)=\frac{1}{q^2}\sum_{s=-\infty}^{\infty}\frac{A_s^\pm}{4s\pm 1-i\gamma}\left[F\left(\frac{q}{4s\pm 1-i\gamma}\right)+F\left(\frac{-q}{4s\pm 1-i\gamma}\right)\right], \quad (24)$$

$$\omega_L=a^2eH^3/4\pi^3Nc\hbar^2y_m^2. \quad (25)$$

The dispersion equation (23) is quite complicated and cannot be solved analytically. The character of its solutions can be investigated by considering the behavior of the functions $\Phi_\pm(q)$. The imaginary part of the functions $\Phi_+(q)$ and $\Phi_-(q)$ coincide, and their real parts differ only in sign. It suffices therefore to consider one of them, for example Φ_+. In the collisionless limit $\gamma \to 0$, the plots of the real and imaginary parts of the function $\Phi_+^0(q)$ at real q are shown in Fig. 2.

In the region $q \ll 1$ we have $\Phi_+^0 \approx q^{-2}$. This branch of the dispersion curve corresponds to a helicon. At a certain value of q less than η^{-1}, the function Φ_+^0 reaches a minimum and tends to infinity as $q \to \eta^{-1}$. Thus, above the helicon threshold there is a solution that describes the DSCR mode due to the resonance of the holes with the maximum displacement. The properties of this wave

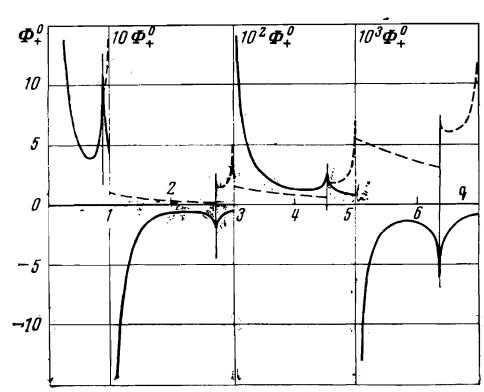

FIG. 2. Dependence of the real (solid curves) and imaginary (dashed curves) parts of the function Φ_+^0 on the reduced wave number q. The ordinate scale is different in different regions of q.

were discussed by Larsen and Greisen[11]. This doppleron is practically unobservable, inasmuch as it exists in the same polarization and in the same field region as the helicon, and its amplitude is much smaller than the helicon amplitude.

In the intervals

$$\eta^{-1}(2k+1)<|\mathrm{Re}\, q|<2k+1 \quad (k=0,1,,2\ldots) \tag{26}$$

the function $I_2(q/(2k+1))$ and $I_3(q/(2k+1))$ have large imaginary parts due to the strong cyclotron absorption of the wave by holes for which $\partial S/\partial k_z$ lies in the interval from $y_m\pi/a$ to $\eta y_m\pi/a$. The existence of the large imaginary part Φ leads to the fact that there are no propagating modes in the intervals (26).

In the gaps between the intervals (26), the imaginary part of I_2 and I_3 are equal to zero, and Im Φ is connected with the imaginary part of I_1, which is small. To the contrary, the quantities $\mathrm{Re}(I_2+I_3)$ have singularities on the boundaries of these gaps, with Re I_2 becoming infinite on the right-hand boundary and Re I_3 on the left-hand boundary. The quantity Re Φ_+ is positive in the intervals

$$4j-1<|\mathrm{Re}\, q|<\eta^{-1}(4j+1) \quad (j=1,2,\ldots) \tag{27}$$

and negative in the intervals

$$4j-3<|\mathrm{Re}\, q|<\eta^{-1}(4j-1) \quad (j=1,2,\ldots). \tag{28}$$

This means that in the intervals (27) there are solutions of the dispersion equation describing the propagating modes with positive polarization, and in the intervals (28) with negative polarization. In each of these intervals there are two solutions.

The regions of existence of all these dopplerons have thresholds on the side of weaker magnetic fields. The values of the threshold fields decrease monotonically with the number of the resonance. As seen from Fig. 2, in the midpoints of the intervals (27) and (28), at magnetic-field values close to the threshold, the imaginary and real parts of the function Φ_+ become of the same order, and therefore in these regions of q there are no propagating solutions. Consequently, the values of the reduced wave numbers $q' = \mathrm{Re}\, q$ of the dopplerons are close to the resonant values. The solutions with $q' \gtrsim 2k+1$ are due to the multiple DSCR of the holes with the minimum displacements, and the solutions with $-q' \lesssim \eta^{-1}(2k+1)$ are due to the multiple resonances of the holes with the maximal $\partial S/\partial k_z$. Since the functions $\Phi_\pm^0(q)$ are even in q, for each solution of the dispersion equation (23) there is a symmetrical solution that differs only in the sign of q'. The physical solution is the one corresponding to the positive group velocity $d\omega/d\kappa$. Such solutions have negative values of q' for dopplerons due to the maximum of $\partial S/\partial k_z$, and positive values of q' for dopplerons due to the minimum of $\partial S/\partial k_z$.

In the vicinities of the resonances, the dispersion equation (23) can be solved approximately. To this end, we represent the variable q in the form $q = q' + iq''$, where q' and q'' are the real and imaginary parts of q. Expanding the expressions in (23) and (24) in terms of the quantities

$$\frac{\gamma}{4s\pm1},\quad \left(q''+\frac{\gamma q'}{4s\pm1}\right)[q'+(4s\pm1)]^{-1},$$
$$\left(q''+\frac{\gamma q'}{4s\pm1}\right)\left[q'+\frac{(4s\pm1)}{\eta}\right]^{-1} \tag{29}$$

and separating the imaginary and real parts, we obtain

$$\omega_L/\omega=\pm\mathrm{Re}\,\Phi_+^0(q'), \tag{30}$$

$$q''=\mp\left\{\frac{d}{dq'}\mathrm{Re}\,\Phi_+^0(q')\right\}^{-1}\left\{\mathrm{Im}\,\Phi_+^0(q')+\frac{\gamma}{q'^2}\sum_{s=-\infty}^{\infty}\frac{A_s^\pm}{(4s\pm1)^2}\left(1+q'\frac{d}{dq'}\right)\right.$$
$$\left.\times\,\mathrm{Re}\left[F\left(\frac{q'}{4s\pm1}\right)+F\left(\frac{-q'}{4s\pm1}\right)\right]\right\}. \tag{31}$$

The solutions of (30) can be obtained, for example, graphically from the intersection of a horizontal line corresponding to the given value of the ratio ω_L/ω with the plot of the function Re $\Phi_+^0(q')$. The dependences of the reduced wave numbers of the dopplerons on the magnetic field are shown in Fig. 3. Positive values of the magnetic field correspond to negative polarization and vice versa. The wavelengths $2\pi/\kappa'$ of the dopplerons due to the minimum of $\partial S/\partial k_z$ are close to $u_{min}/(2k+1)$, while the wavelengths due to the maxima of $\partial S/\partial k_z$ are close to $u_{max}/(2k+1)$.

It is seen from (31) that the damping of the dopplerons depends strongly on the value of the derivative $d\,\mathrm{Re}\,\Phi_+^0/dq'$. In the strong-field region, where the derivative increases without limit, the nonlocal damping tends to zero. The total damping tends to $\kappa'' = l^{-1}$, where l is the mean free path of the resonant carriers. With decreasing magnetic field, the derivative $d\,\mathrm{Re}\,\Phi_+^0/dq'$ decreases, while the nonlocal damping increases and becomes infinite at the threshold field value. Therefore the region where the doppleron can be observed is bounded on the weak-field side by a field value slightly exceeding the threshold.

The character of the variation of the collisional part of the damping with decreasing field depends on the type of the wave. If we consider in (30), (31), and Φ_+^0 only one term with number s, then when the field is decreased the collision part of the damping decreases for the doppleron due to the minimum of $\partial S/\partial k_z$, and increases for the doppleron due to the maximum of $\partial S/\partial k_z$. Therefore a correct allowance for the collision damping shows that the lower limit of the region of the observation of the doppleron due to the minimum of $\partial S/\partial k_z$ is somewhat lower, while that of the doppleron due to the maximum of $\partial S/\partial k_z$ is somewhat higher, than that obtained if one neglects the dependence of the collision damping on the field ($\kappa''_{col} = l^{-1}$). The influence of the remaining terms in (31) complicates the picture. For the assumed model with parameters (5) it turns out that a correct allowance for the collision damping for all the dopplerons due to the maximum of $\partial S/\partial k_z$ raises the lower limiting field, and consequently narrows down the observation region. For the first and third dopplerons due to the minimum, the boundary drops and the region of observation broadens, while for the fifth doppleron the boundary rises.

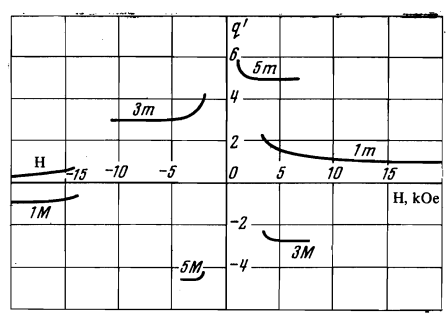

FIG. 3. Dependence of the real parts of q on the magnetic field intensity at f_0 = 200 kHz. The curve H corresponds to the helicon; the curves 1m, 3m, and 5m correspond to multiple dopplerons due to the minimum of $\partial S/\partial k_z$; the curves 1M, 3M, and 5M correspond to multiple dopplerons due to the maximum of $\partial S/\partial k_z$.

D. Impedance of Plate

The character of reflection of carriers from the surface of the metal has very little effect on the behavior of the amplitude of the transmitted wave when the field is altered [8], so that in the calculation of the impedance we shall deal with the simpler case of specular reflection. For a thick plate ($\kappa''d \gtrsim 1$), neglecting the waves reflected from the surface, the contribution made to the derivative of the surface impedance of the plate, due to the propagation of a doppleron in the plate, is given by [7]

$$\frac{d\Delta Z}{dH} \sim \exp\left(-q''H\frac{2ead}{c\hbar y_m}\right)\frac{d}{dH}\left\{\frac{H^2}{q'^2}\left(\frac{d\,\mathrm{Re}\,\Phi_\pm{}^0}{dq'}\right)^{-1}\exp\left(iq'H\frac{2ead}{c\hbar y_m}\right)\right\}, \tag{32}$$

where $q'(H)$ is the solution of Eq. (30) and d is the thickness of the plate.

With changing magnetic field, the impedance of the plate experiences oscillations whose period is equal to

$$\Delta H = \Delta H_{GK}\left|q' + 3\,\mathrm{Re}\,\Phi_\pm{}^0(q')\left(\frac{d\,\mathrm{Re}\,\Phi_\pm{}^0(q')}{dq'}\right)^{-1}\right|^{-1}, \tag{33}$$

where

$$\Delta H_{GK} = \pi\hbar c y_m/ead \tag{34}$$

is the period of the Gantmakher-Kaner oscillations [2]. In the region of strong fields, where $d\,\mathrm{Re}\,\Phi_\pm^0(q')/dq'$ tends to infinity, the period ΔH approaches $\Delta H_{GK}/(2k+1)$ for dopplerons due to the minimum of $\partial S/\partial k_z$, and approaches $\eta\Delta H_{GK}/(2k+1)$ for dopplerons due to the maximum of $\partial S/\partial k_z$. With decreasing field, the period of the doppleron oscillations due to the minimum increases, as seen from formula (33) and Fig. 2, and the period of the oscillations due to the maximum decreases. For the model parameters assumed by us, these tendencies remain in force for the entire region of doppleron observation, although generally speaking they could change in still weaker fields. Plots of $\Delta H/\Delta H_{GK}$ are shown in Fig. 4.

The doppleron observation region is bounded on the weak-field side by the damping q''. In strong fields the amplitude of the oscillations decreases because of the increase of the derivative $d\,\mathrm{Re}\,\Phi_\pm^0/dq'$. When the field increases from the threshold value, the amplitude of the oscillations of the derivative of the surface resistance $d(\Delta R)/dH$ increases, reaches a maximum, and then decreases. The oscillations for a plate of thickness d = 0.50 mm, frequency $f = \omega/2\pi = 200$ kHz, and $\gamma = 1/H$ kOe ($\nu mc/e = 10^3\ g^{1/2}\,cm^{-1/2}\,sec^{-1}$) are shown in Fig. 5. It is seen from the figure that the regions where dopplerons oscillations are observed are monotonically lowered with increasing number of the resonance. For dopplerons due to the maximum, they are very narrow and contain two or three oscillations, and the amplitudes of these oscillations are relatively small. For dopplerons due to the minimum, the region of optimal observation includes many oscillations. The maximal values of the amplitudes of these oscillations decrease monotonically with the number of the doppleron.

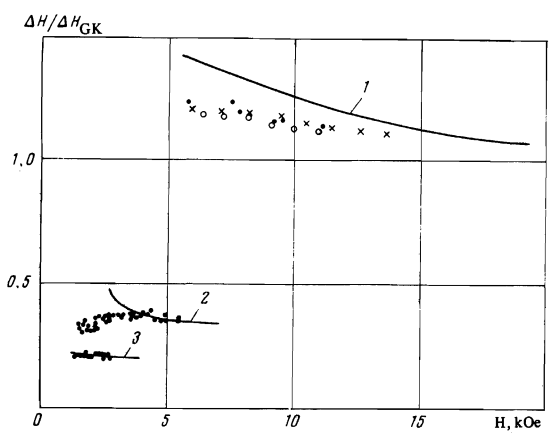

FIG. 4. Dependence of the reduced period of the doppleron oscillations on the magnetic field at a frequency $f_0 = 200$ kHz and $\partial S/\partial k_z = 8.1\ (\pi/a)\ \text{Å}^{-1}$. Curves—results of calculation. The experimental data for the first harmonic, for samples with different thicknesses d, are marked by different symbols ○—d = 0.51 mm, X—d = 0.46 mm, ●—d = 0.31 mm. For the third and fifth harmonics, the results for all samples are represented by points.

3. EXPERIMENT

A. Measurement Procedure and Samples

The DSCR was investigated experimentally on aluminum samples having resistance ratios $\rho_{300°K}/\rho_{4.2°K} = 7 \times 10^3$. The samples were single-crystal plates measuring 10×4 mm and 0.31, 0.46, and 0.51 mm thick. They were cut by the electric spark method from a single-crystal cylinder. The sample orientation was determined by x-ray diffraction. The normal to the plane of the plate was directed along the [100] axis with accuracy of approximately 1°. The samples were etched in a solution of nitric acid. The surface of the plate had no mirror brilliance after the etching.

As shown by the investigations of [8-10], the use of circular polarizations in the case of a magnetic field normal to the surface of the sample is a convenient method of investigating DSCR and the dopplerons associated with it. This method makes it possible to distinguish the impedance oscillations due to doppleron excitation from the Gantmakher-Kaner oscillations, and also makes it possible to investigate the impedance singularities produced in a semi-infinite metal by the propagation of dopplerons. Therefore, in the investigation of the DSCR in aluminum, the exciting radio-frequency field was circularly polarized. The sample was securely mounted in two flat mutually perpendicular coils. One of the coils was the inductance coil of the tank circuit of an autodyne detector with constant sensitivity [16]. The second was used to produce a radio-frequency field having a circular polarization in the plane of the sample. The direction of the rotation of the electric and magnetic vectors of the field could be varied in the course of the measurements. The measurements were performed in a magnetic field of intensity up to 16 kOe, which was produced by an elec-

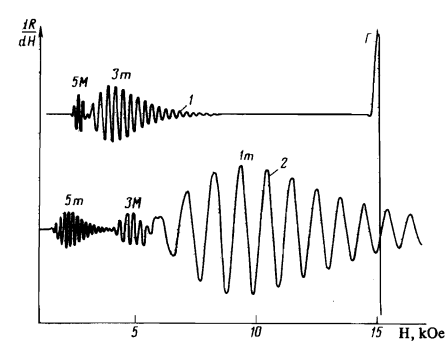

FIG. 5. Calculated plots of the derivative of the surface resistance against the magnetic field in the case of positive (curve 1) and negative (curve 2) polarization at a frequency $f_0 = 200$ kHz and a plate thickness d = 0.50 mm.

tromagnet. The field of the magnet was modulated in amplitude at a frequency 10 Hz. The modulation amplitude reached 120 Oe. The autodyne signal was proportional to the derivative dR/dH of the surface resistance with respect to the magnetic field, and was fed after amplification and synchronous detection to the Y input of an automatic X-Y potentiometer. The X input was the voltage from a Hall pickup, which was calibrated against NMR signals with a running-water magnetometer [17] directly during the course of the measurements. The total error in the plot of dR/dH did not exceed 1%. The measurement procedure was described in greater detail earlier [7,8,16].

The measurements were performed in the frequency interval 0.15—2.0 MHz at a temperature 4.2°K. Further lowering of the temperature did not lead to an increase of the observed dR/dH oscillations. The direction of the magnetic field, parallel to the binary axis [100] of the crystal, was determined at the start of each experiment from the symmetry of the angular dependence of $R(\theta)$, where θ is the angle in the crystallographic plane (010) of the sample between the direction of the magnetic field and the [100] axis. The amplitude and the phase of the voltage on the auxiliary coil were then adjusted to obtain circular polarization of the exciting field. After determining the orientation of the magnetic field and selecting the polarization, we plotted dR/dH at positive and negative polarizations.

B. Measurement Results

Typical plots of the derivatives $dR_{\pm}/dH$ in a wide interval of magnetic fields are shown in Fig. 6a. Against the background of smooth variations of the derivatives, one can see four series of oscillations, marked on the figure by the letters A, B, C, and H. The oscillations H were observed in strong magnetic fields in positive polarization and are due to helicon excitation. The threshold field of the helicon, proportional to $f^{1/3}$, had a value $H_L = 12.3$ kOe at the frequency f = 175 kHz. The helicon dispersion in aluminum was investigated in detail by Larsen and Greisen [11].

The oscillation series A, B, and C exist in limiting magnetic-field intervals. The upper and lower limiting fields for these types of oscillations increase with increasing frequency in proportion to $f^{1/3}$. The periods of the oscillations did not depend on the frequency, so that to observe a large number of oscillations of the series

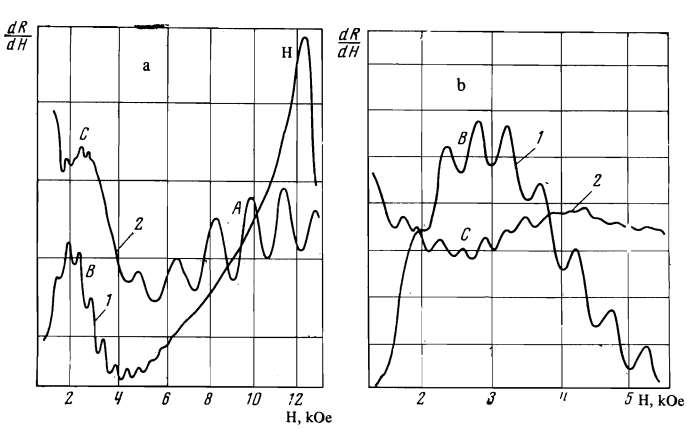

FIG. 6. Plots of $dR_{\pm}/dH$ against the magnetic field for samples of thickness d = 0.31 mm: a—frequency f = 170 kHz, b—510 MHz; T = 4.2°K. Curves 1 and 2 correspond to polarization plus and minus, respectively. The plots for equal frequencies were drawn at equal gains.

A, B, and C it is advisable to perform the measurements at higher frequencies. However, an increase of the frequency above 1 MHz has led to a decrease in the amplitudes of the oscillations, probably owing to the quality of the sample surface. Figure 6b shows plots for the same sample as in Fig. 6a, but at a larger gain and at a frequency f = 510 kHz.

The A oscillations have the largest amplitude and are observed only at negative polarization. They exist in a wide range of magnetic fields both below and above the helicon threshold. The B oscillations are observed in positive polarization and in weaker magnetic fields, and their amplitude is lower than that of the A oscillations. The C oscillations have negative polarization, the lowest amplitude, and the narrowest region of existence with respect to the magnetic field. We make no quantitative comparison of the amplitudes of the different types of oscillations, in view of the dependence on the thickness of the samples, on the frequency, and on other factors.

As seen from Fig. 6, the A, B, and C oscillations are approximately periodic in the magnetic field and their periods vary slowly with changing field intensity. Figure 4 shows the results of the measurements of the dependence of the periods of three types of oscillations on the magnetic field for samples with different thicknesses. The ordinates in this figure represent the ratio $\Delta H/\Delta H_{GK}$, where ΔH is the distance over the magnetic field between the two neighboring maxima of the given group of oscillations, and ΔH_{GK} is the period of the Gantmakher-Kaner oscillations (see (34)) for the sample of the corresponding thickness and the value $\partial S/\partial k_z = 8.1(\pi/a)\text{Å}^{-1}$. The abscissas represent the values of $H(f_0/f)^{1/3}$, where f is the frequency at which the measurements were made, $f_0 = 200$ kHz, and H is the arithmetic mean of the magnetic fields corresponding to the maxima.

As seen from the foregoing results, the value of $\Delta H/\Delta H_{GK}$ does not depend on the sample thickness, i.e., the periods of the A, B, and C oscillations are inversely proportional to the thickness d. The period of the A oscillations, in the entire region where they are observed, decreases smoothly with increasing magnetic field. The maximum change of the period is 12%, in agreement with the results of Larsen and Greisen [11]. In weak fields, the period of the B oscillations increases with increasing magnetic field. In stronger fields, it seems to decrease on going through the maximum, although the spread of the experimental points does not make it possible to reject another possibility, namely, that starting with a certain field H_0 the period assumes a constant value. With the same accuracy, it can be stated that the period of the C oscillations is independent of the field. The periods of the A, B, and C oscillations are approximately multiples of one another and their ratio is 1 : 1/3 : 1/5. The magnetic field regions in which the oscillations are observed can be determined from the experimental data are shown in Fig. 4. We note also that the amplitudes of the oscillations are very sensitive to the orientation of the magnetic field. When the field deviates from the direction of the normal to the sample surface, the amplitudes decreases sharply, and more abruptly for the B and C oscillations than for the A oscillations. At $\vartheta \geq 5°$, the B and C oscillations were not observed. The decrease of the amplitudes is connected with the strong anisotropy of the Fermi surface.

The properties of the A, B, and C oscillations, namely their existence only in a definite circular polarization,

the limited region of magnetic fields in which they are observed, and the dependence of the period in the field, allow us to state that they are due to the propagation of dopplerons which are connected with multiple DSCR, and not with the Gantmakher-Kaner size effect, as was assumed in [12]. The multiple dopplerons should exist in aluminum, since its Fermi surface does not have axial symmetry. In accordance with the doppleron theory developed in Sec. 2, the period of the doppleron oscillations in strong magnetic fields is close to the corresponding multiple period of the GKO. According to the experimental data and formula (34), for the GKO there were obtained the following values of $\partial S/\partial k_z$ of the resonant group of carriers, in accordance with the measurements of different harmonics: for the first harmonic $dS/\partial k_z = (9.0 \pm 0.5)(\pi/a)$ Å^{-1}; for the second and third harmonics $(8.6 \pm 0.5)(\pi/a)$ Å^{-1} and $(8.3 \pm 0.5)(\pi/a)$ Å^{-1}, respectively. The large value of $dS/\partial k_z$ for the first harmonic seems to be connected with the fact that the period of oscillations does not reach the limiting value in the region where the fundamental doppleron is observed. For the third and fifth harmonics, the period of the oscillations has a smaller dispersion and is close to the corresponding GKO period. We believe that the value of $\partial S/\partial k_z$ of the resonant group of the holes at the minimum is $(8.1 \pm 0.5)(\pi/a)$ Å^{-1}.

In addition to the aforementioned singularities of the derivatives of the surface resistance, in still weaker fields one observes several dR_+/dH oscillations of small amplitude, the period of which is approximately 1/9 of the period of the A oscillations.

4. DISCUSSION

A comparison of the theory of multiple dopplerons and of the experimental results shows that they are in qualitative agreement. The theoretically predicted polarizations of the multiple dopplerons and the experimentally observed polarizations agree. In strong fields, the theoretical and experimental ratios of the limiting periods of the different types of oscillations also agree. As seen from Figs. 4—6, the magnetic-field regions in which the phenomena are observed, as well as the amplitude ratio of the first and fifth dopplerons, are close to those given by the theory. The region of observation of the third doppleron lies in weaker fields than would follow from our theory. The dispersion of the period of the A and C oscillations is described qualitatively correctly by the theoretical curves 1 of Fig. 4, which pertain to the first and fifth dopplerons. No such statement can be made concerning the B oscillations. As already mentioned, the dispersion of the periods of the dopplerons is very sensitive to the choice of the model. In addition, the quantitative ratios of the amplitudes of the different dopplerons and the regions of their observations are also determined to a considerable degree by the parameters of the model. The characteristic features of the fundamental resonance depend mainly on the behavior of the function $\partial S/\partial k_z$ in the vicinity of its minimum, whereas the properties of the higher harmonics depend on the fine details of the Fermi surface, namely on the character of the variation of $\partial S/\partial k_z$ in the entire Brillouin zone, on the corrugation and its variation with k_z, etc. Since the Fermi-surface model chosen by us is quite simple and describes only qualitatively the shape and dimensions of the real Fermi surface, one can hardly expect a complete quantitative agreement between our theory and experiment. We see nevertheless that even such a simple model describes the greater part of the characteristic features of the DSCR in aluminum.

Thus, it follows from our results that the oscillations with multiple periods, observed in aluminum, are due to the propagation of multiple dopplerons. In light of this, the statement made by Falk [15] that it is impossible to observe multiple DSCR modes is incorrect. The amplitudes of the multiple harmonics, even though they decrease monotonically with the number, remain sufficiently large and are observed in the experiment.

The aforementioned oscillations of dR_+/dH with a period approximately equal to 1/9 of the period of the fundamental doppleron may constitute the ninth harmonic of the DSCR of the holes with the minimum displacement u_{min}. It is more probable, however, that these oscillations are connected with excitation of a doppleron due to another group of carriers, located at $k_z \approx 1.7\ \pi/a$ Å^{-1} and having a displacement $u \approx u_{min}/9$ (see curve 3 in Fig. 1).

It should be noted in conclusion that impedance oscillations with multiple periods were observed earlier in indium [18], the Fermi surface of which is similar to that of aluminum. The oscillations corresponding to the third harmonic of the DSCR were observed in both circular polarizations, although they differed somewhat in amplitude and in shape [9]. In light of the results of Sec. 2D of the present paper, we can suggest that the oscillations of the third harmonic in the positive polarization are connected with the excitation of a doppleron due to DSCR of holes with minimum displacement, whereas the oscillations in the negative polarization are due to DSCR of holes having the maximum displacement.

The authors are grateful to V. G. Fastovskiĭ for interest in the work and to N. N. Mikhaĭlov for preparing the aluminum single crystals.

[1] O. V. Konstantinov and V. I. Perel', Zh. Eksp. Teor. Fiz. **38**, 161 (1960) [Sov. Phys.-JETP **11**, 117 (1961)].
[2] V. F. Gantmakher and É. A. Kaner, Zh. Eksp. Teor. Fiz. **48**, 1572 (1965) [Sov. Phys.-JETP **21**, 1053 (1966)].
[3] J. C. McGroddy, J. R. Stanford, and E. A. Stern, Phys. Rev. **141**, 437, 1966.
[4] A. W. Overhauser and S. Rodriguez, Phys. Rev. **141**, 246, 1966.
[5] R. G. Chambers and V. G. Skobov, J. Phys. **1**, 202, 1971.
[6] D. S. Falk, B. Gerson, and J. F. Carolan, Phys. Rev. **B1**, 407, 1970.
[7] L. M. Fisher, V. V. Lavrova, V. A. Yudin, O. V. Konstantinov, and V. G. Skobov, Zh. Eksp. Teor. Fiz. **60**, 759 (1971) [Sov. Phys.-JETP **33**, 410 (1971)]; Zh. Eksp. Teor. Fiz. **63**, 224 (1972) [Sov. Phys.-JETP **36**, 118 (1973)].
[8] V. V. Lavrova, S. V. Medvedev, V. G. Skobov, L. M. Fisher, and V. A. Yudin, Zh. Eksp. Teor. Fiz. **64**, 1839 (1973) [Sov. Phys.-JETP **37**, 929 (1973)].
[9] V. V. Lavrova, V. G. Skobov, L. M. Fisher, A. S. Chernov, and V. A. Yudin, Fiz. Tverd. Tela **15**, 3379 (1973) [Sov. Phys.-Solid State **15**, 2245 (1974)].
[10] V. V. Lavrova, S. V. Medvedev, V. G. Skobov, L. M. Fisher, A. S. Chernov, and V. A. Yudin, Zh. Eksp. Teor. Fiz. **66**, 700 (1974) [Sov. Phys.-JETP **39**, 338 (1974)].

[11] P. K. Larsen and F. C. Greisen, Phys. Stat. Sol., b, **45**, 363, 1971.
[12] S. Balibar, B. Perrin, and A. Libchaber, J. Phys., **F2**, 4629, 1972.
[13] C. O. Larson and W. L. Gordon, Phys. Rev. **156**, 703, 1967.
[14] E. A. Kaner and V. G. Skobov, Adv. in Phys. **17**, 605, 1968.
[15] D. S. Falk, Phys. Rev. **B3**, 1973, 1971.
[16] V. A. Yudin and L. M. Fisher, Prib. Tekh. Éksp. No. 3, 131 (1971).
[17] V. A. Yudin, Prib. Tekh. Éksp. No. 6, 188 (1967).
[18] I. P. Krylov, Zh. Eksp. Teor. Fiz. **54**, 1738 (1968) [Sov. Phys.-JETP **27**, 934 (1968)].

Translated by J. G. Adashko
134